Assessing the role of climate factors on malaria transmission dynamics in South Sudan

Abdulaziz Y.A. Mukhtar[1,2*], Justin B. Munyakazi[1], and Rachid Ouifki[3]

[1]Department of Mathematics and Applied Mathematics, University of the Western Cape, Private Bag X17, Bellville 7535, South Africa
[2]DST-NRF Centre of Excellence in Mathematical and Statistical Sciences (CoE-Mass)
[3] Department of Mathematics and Applied Mathematics, Faculty of Natural & Agricultural Sciences, University of Pretoria, Private Bag X20, Hatfield 0028, South Africa

January 20, 2019

Abstract

Malaria is endemic in South Sudan and it is one of the most severe diseases in the war-torn nation. There has been much concern about whether the severity of its transmission might depend upon climatic conditions that are related to the reproduction of the single-cell parasite attaching to female mosquitoes, especially in high altitude areas. The country experiences two different climatic conditions; namely one tropical and the other hot and semi-arid. In this study, we aim to assess the potential impact of climatic conditions on malaria prevalence in these two climatically distinct regions of South Sudan. We develop and analyze a host-mosquito disease-based model that includes temperature and rainfall. The model has also been parameterized in a Bayesian framework using Bayesian Markov Chain Monte Carlo (MCMC). The mathematical analysis for this study has included equilibria, stability and a sensitivity index on the basic reproduction number $\mathcal{R}_0$. The threshold $\mathcal{R}_0$ is also used to provide a numerical basis for further refinement and prediction of the impact of climate variability on malaria transmission intensity over the study region. The study highlights the impact of various temperature values on the population dynamics of the mosquito.

Keywords: Malaria, Basic reproduction number, climate, Bayesian approach.

[0]*Corresponding author. E-mail: amukhtar@uwc.ac.za.

1 Introduction

Malaria is the most prevalent human mosquito-borne disease caused by a single-cell parasite that infects female Anopheles mosquitoes [4, 13]. This disease remains one of the biggest health threats facing humanity and is transmitted more robustly and incessantly in Sub-Saharan Africa than it is elsewhere. The Republic of South Sudan (RSS), the youngest country with civil unrest is one of the countries in Sub-Saharan Africa that is severely confronted by malaria. There have been approximately 1.54 million malaria episodes and almost 718 deaths reported in 2014, with 65% of those being children [34]. Moreover, malaria is endemic within the country [34]. However, little is known about local environmental conditions that may contribute to the severity of the disease during wet seasons. Improving our perception of host-parasite interactions in the war-torn nation is a priority in which mathematics can bring insight, especially regarding conjectures that attribute this gravity to climatic factors.

The malaria parasite depends upon the Anopheles mosquito to supplement its life cycle through a human intermediary. This relationship means that a climatic influence on mosquitoes' bionomics will trigger the trend towards malaria that is most likely to follow the climatic pattern, especially in the endemic zone. For this reason, an increase in mosquito density leads to a higher risk of malaria prevalence. For instance, Abiodun and Ewing [2, 11] have recently revealed that climate fluctuations not only have a reproducible effect on the mosquito lifespan, but also impact positively on the development of sporogonic stages of the malarial parasite within the mosquito's body. Warmer temperature increases mosquito activity and more rainfall can lead to an abundance of mosquito larvae [4, 5, 17, 28]. Thus, the use of mean temperatures might be appropriate under certain conditions, which are generally found to have significant implications in determining the risk of malaria [6, 33].

Similar research [29, 36] has shown that mosquitoes are particularly active at dusk and dawn, while prolonged sun exposure can lead to their dehydration. Little is known about the survival of mosquito-borne diseases and malaria transmission during the winter, however, it is often noted that mosquitoes tend to disappear in winter or when temperatures drop below 10°C. Nonetheless, the vertebrate host is the immediate source of winter infection in mosquitos, since the virus simply survives in the cold weather, waiting for warmer weather to reproduce. According to a study by [36] female mosquitoes spawn tumblers, which ultimately freeze in winter (or at temperatures below 10°C). The frozen eggs are saved until the temperature warms, when mosquito proliferation begins again, with disastrous effects on humans. These findings point to the effect of changes in ambient temperatures and precipitation levels on mosquito populations and thus stimulates interest in understanding the impact of these factors on mosquito-borne disease transmission.

In South Sudan malaria transmission is alleged to be perennial across the country, with peaks towards the end of the rainy season from September to November [14, 23], as freshwater pools become mosquito breeding sites. The country has two different climatic conditions, a hot semi-arid climate and a tropical climate. It is observed that malaria prevalence is significantly higher in the southern region (a tropical region, i.e., Central Equatorial State

(CES)) than it is in northern region (a hot semi-arid region, i.e., Western Baher El Ghazal State (WBZ)) as is illustrated in Figure 1. The disease prevalence could be as high as 75% to 100% in some counties in the South. It is still uncertain, and a matter of discussion, whether and how the changes in transmission might occur. Understanding the dynamics of mosquito population is crucial for gaining insight into the abundance of mosquitoes, and thus design operational strategies for control. With this backdrop, we endeavor to understand the exact role that climate plays on the transmission of malaria in two different climatic zones of South Sudan through mathematical modelling. The CES and WBZ States are chosen (one from each climatic zone) due to the severity of malaria within their region. This is the first study designed for this purpose in CES and WBZ since the call for the implementation of the malaria control program.

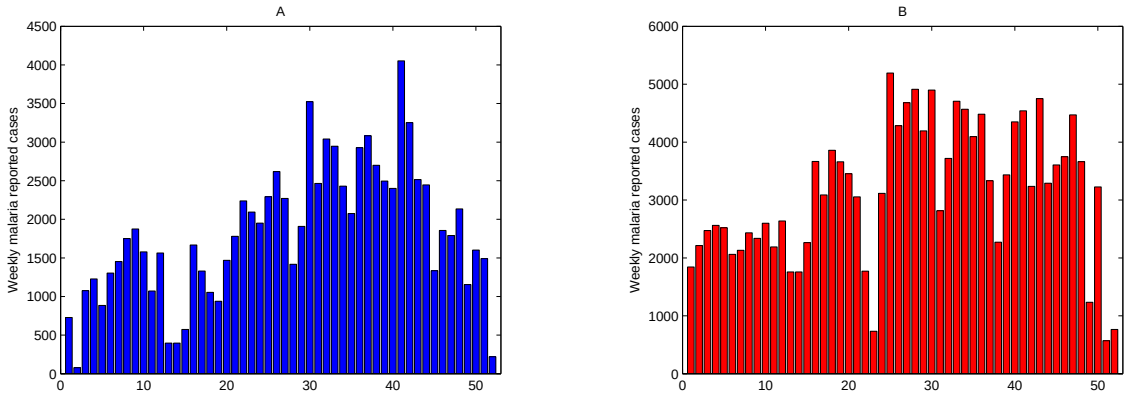

Figure 1: Weekly malaria reported cases of 2015 for (A) Western Baher el Ghazal State (in region 2) and (B) Centeral equatorial State (in region 1)

A number of studies using mathematical models have established the direct role that climate variables, such as temperature and rainfall, play in the transmission dynamics of vector-borne diseases [1, 4, 10, 11, 16, 20, 22, 28, 33, 40]. Yang [40] presented a malaria transmission model by taking into account different levels of acquired immunity among humans and, most importantly, temperature-dependent parameters related to vector mosquitoes. A model analysis was carried out by means of the basic reproduction number R_0. Additionally, an expression was derived for an endemic equilibrium that is biologically relevant only when $R_0 > 1$. Hoshen and Morse [16] formulated a dynamic malaria model comprising both the weather-dependent within-vector stages and the weather-independent within-host stages. Martens et al. [22] used rules-based modelling approach to examine how climate change might affect global malaria transmission. Their model consists of several linked systems: the climate system, the malaria system (divided into a human subsystem and a mosquito subsystem), and the impact system. Birley [20] presented a simple mathematical model to investigate the effects of temperature on the ability of Anopheles maculipennis to transmit Plasmodium vivax malaria.

In recent decades also several contributions have been made in Africa concerning the distribution of mosquitoes affected by various environmental (climatic) factors such as temperature, humidity, rainfall and wind [2, 3, 12, 17, 18, 21, 30, 38, 39]. For instance, Parham et al. [30] developed an integrated modeling framework for assessing and predicting the simultaneous effects of rainfall and temperature on malaria dynamics. They illustrated the role that large-scale climate simulations and infectious disease systems may provide in predicting changes in the basic reproduction number across Tanzania. This offers powerful tools for understanding geographic shifts in incidence as climate changes. Yamana et al. [38] assessed the influence of climate change on malaria transmission in West Africa. Their simulation results stated that the changes in the pattern of rainfall play a significant role on malaria transmission compared to the potential impact of rising temperatures. They suggest that it will be necessary to integrate the changes in rainfall pattern in order to accurately project the environmental suitability for malaria transmission in future climates. Lunde et al. [21] formulated a realistic representation of Anopheles Gambiae s.s. and Anopheles Arabiensis in order to ameliorate the understanding of the dynamics of these vectors. Their study highlight how parameters can influence the success of these two species, as temperature, relative humidity and mosquito size are essential aspects in malaria transmission.

In spite of these studies, most modellers often ignore to validate their climate-based models with field data in order to carry out a quantitative assessment of the human component of the model. The aim of this study is to assess the impact of temperature and rainfall on the dynamics of mosquito population of a certain region of South Sudan and taking into consideration the climate-driven dynamics model. In addition, we further consider the importance of evaluating the numerical values of the model paramters with real data in order to allow for a computational simulation of dynamics that provides accurate prediction of the reaction.

Without accurate predictions, calculations of the basic reproduction number which explains the capability of a disease to persist in a population, will be subject to a significant error. This may help in a better understanding of the regulations of the biological system of the disease that can help decision-makers in developing efficient intervention strategies to tackle the disease. Therefore, the model framework is designed to accommodate human-mosquito population dynamics and to estimate its parameters using the Bayesian approach. Bayesian approaches, in particular Markov Chain Monte Carlo (MCMC) turn out to be a powerful inference tool for complex systems raised in behavioral science and computational biology [15, 41]. The input data required to validate our model are malaria incidence cases at state level in each region for a given period of time. The climate data are obtained from [35] and Regional Meteorological Service [7].

2 Spatial trends

According to Köppen and Geiger, South Sudan has two different climates [32]:
(i) A tropical savanna climate which is characterized by a rainy season of high humidity followed by a dry season with mild temperatures ranging from an average minimum of 20°C

to a maximum of 38°C [32], (ii) A hot semi-arid climate characterized by a more moderate summer temperature regime, with daily mean temperatures of around 19°C. The study is conducted in two climatically distinct regions: Equatorial region and Baher El Ghazal region. A map of the study area is provided in Figure 2. The seasonal changes in these environments drive a strong vectorial capacity that sustains high levels of transmission. Our study domain is determined by longitude and latitude, which is interpolated to the spatial resolution data. These two distinct regions are described as:

Region (1): The Southern Part of the country is characterized by an equatorial (tropical) climate, forested, with comparatively lower refugee migration flows, but with some seasonal migration related to agricultural work. This region is divided into 241 counties and mostly comprised of greenbelt, hills and mountains. Average rainfall is between 901 and 1800 mm annually, with the longest rainy season lasting from 7–8 months, as can be seen in Figure 2(right). Humid conditions and a relatively warm climate make this region conducive to the reproduction of mosquitos. Our study focuses on the Central Equatorial State (CES) as a representative of this region.

Region (2): The northern part of the country is divided into 128 counties and has a climate that is classified as hot and semi-arid. The landscape features western and eastern flood plains that slope gently towards the rivers. Annual average rainfall ranges from between 400 to 600 mm and the duration of the rainy season is from 5–6 months (see Figure 2(right)). Our study focuses on the Western Baher El-Ghazal State (WBGZ) as a representative of this region.

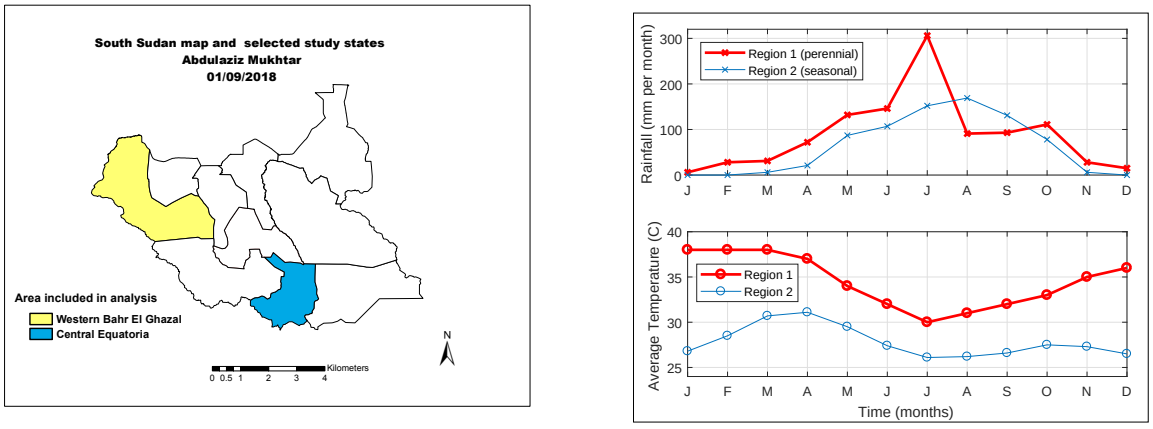

Figure 2: South Sudan States Map (left) and Average rainfall and Temperature for CES & WBGZ (right)

3 Method

We begin with the formulation of a classical epidemiological model that considers human and mosquito populations. The model structure is similar to that of [26] that includes a realistic, climate-based model for capturing the simultaneous effects of rainfall and temperature on malaria transmission. The human component is utilized to fit the model to the actual observed data via a Bayesian approach. Both components of the model are used simultaneously to estimate mosquito bite rate that is assumed to be influenced by LLINs intervention coverage and not climate-dependent. We hence end this section by applying a Bayesian approach to estimate the posterior distribution of parameters given actual-settings data.

3.1 Model formulation

Based on the foregoing and established studies, we presume the heterogeneity of malaria in South Sudan can be explained by the varied agro-climatic conditions that exist between the regions. Consequently, we slightly extend the model in [26] by using a deterministic compartmental structure for the endemic malaria disease incorporating the climate factor that leads to understanding the impact of temperature and rainfall. This compartmental model captures the situations including intervention coverage and allows to calibrate parameters against the real observed data. The human components of the model is presented to capture the relationship between effective treatment and parasitic prevalence. The total mosquito population N_M is divided into aquatic mosquitoes (egg, larva and pupa) stage denoted by M and adult mosquitoes N_V. The adult mosquitoes is sub-divided into susceptible mosquitoes S_v, mosquitoes exposed to malaria parasite E_v and infectious mosquitoes I_V. In model formulation, we assume all variables represented in each compartments are differentiable with respect to time and all parameters are non-negative. As illustrated in the flow digarm (Figure 3.1) the total population of humans and mosquitoes at time t will be:

$$N_H(t) = S_H(t) + E_H(t) + I_H(t) + R_H(t);$$

and

$$N_M(t) = M(t) + N_V(t)$$

respectively.

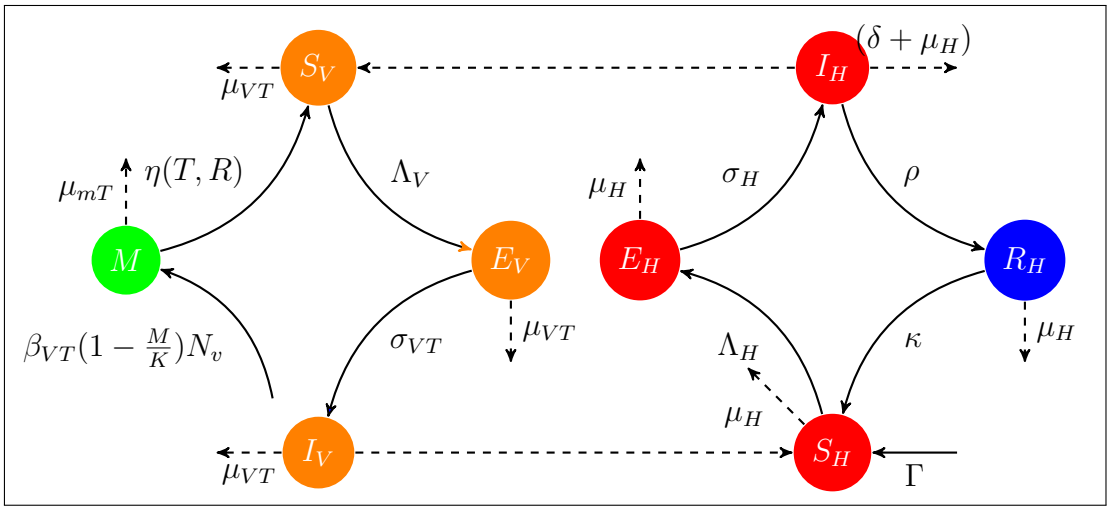

Figure 3: **Flow diagram for Human and Mosquito infection model**

The susceptible compartment is recruited by birth into the community at a rate Γ and increased with recovery rate κ when individuals loose their immunity. We presume susceptible individuals (S) acquire malaria and become infected at a rate Λ_H when they are bitten by infectious mosquitoes (entomological inoculation rate; EIR). After bites from infectious mosquitoes, individuals move to the exposed humans compartment. The exposed human population remains exposed for a fixed number of days as the parasites still in the asexual stages in their bodies before moving to infected humans with probability σ_H. On infection, they develop clinical infection in which they have gametocytes in their bloodstream. Those that are developing disease either die (naturally or due to the disease with probability δ) or successfully recovered (naturally or with treatment) with rate ρ and subsequently enter a period of prophylaxis (recovery state R). Upon treatment intervention, the rate ρ is determined by the proportion of treatment access π, duration of drug recovery period ν and treatment seeking period τ, hence is given by $\rho = (1 - \pi)/\gamma + \pi/(\nu + \tau)$, where γ is natural recovery period. Those who are recovered either lose their immunity and return to susceptible class or naturally die. The deterministic model for the human dynamics is as follows

$$\begin{cases} \dfrac{dS_H}{dt} = \kappa\, R_H - \Lambda_H\, S_H - S_H \mu_H + \Gamma, \\ \dfrac{dE_H}{dt} = \Lambda_H\, S_H - (\mu_H + \sigma_H)\, E_H, \\ \dfrac{dI_H}{dt} = \sigma_H E_H - (\mu_H + \delta + \rho)\, I_H, \\ \dfrac{dR_H}{dt} = \rho\, I_H - (\mu_H + \kappa)\, R_H, \end{cases} \tag{3.1}$$

where t represents time and the force of infection Λ_H is assumed to vary by degree of exposure to mosquito due to geographic variation, governed by the function

$$\Lambda_H = \frac{\epsilon \beta_{HV} I_V}{N_H},$$

where $\epsilon = (1 - V\chi)\epsilon$ is mosquito biting rate that is assumed to be influenced by LLINs intervention coverage, β_{HV} is the probability of infection if bitten by an infectious mosquito.

We consider Anopheles Gambiae mosquitoes which is the main anopheles species that transmits Plasmodium Falciparum in South Sudan to be included in the model. We model a life cycle of mosquito in a compartmental formulation [19], starting with aquatic mosquitoes stages, eggs, larvae and pupae grouped into a single compartment M and further subdivide adult mosquito into three compartments. When Adult mosquitoes lay eggs at rate β_{VT} which is temperature dependent, the aquatic (immature) mosquitoes population is then produced at the temperature and rainfall-dependent rate $\beta_{VT}(1 - M/K)$ [31, 26], by the usage of the carrying capacity parameter K for limitation of the immature mosquito population that depend on habitat availability. The immature mosquito population develop into adult mosquitoes at the birth rate $\eta(T, R)$ which is dependent on temperature- and rainfall and also decreases by natural death rate $\mu_i(T)$. Figure 9 illustrates the effect of climate on these parameters of immature mosquitoes.

Thereafter, adult mosquito population is subdivided into three compartments: susceptible S_V, latent infected E_V and infectious I_V. Susceptible female mosquitoes emerge from the last immature stage at the birth rate adapted from [31, 26] as

$$\eta(T, R) = \frac{\varpi(T) p_i(R) p_2(T)}{\tau_{EA}(T)},$$

where $\varpi(T)$ is the total number of eggs laid per adult per oviposition which is temperature dependent, and $p_i(R)$ is the daily survival probability of immature in stage i given rainfall R (where $i = 1, 2$, and 3 corresponds to eggs, larvae, and pupae respectively). It is assumed that survival probability of eggs and pupae are independent of temperature [12, 31] and $p_2(T) = \exp(-(0.00554T - 0.06737))$ is daily survival probability of the temperature dependent larvae. The total development time of immature mosquito, denoted by $\tau_{EA}(T)$ is given by $1/(-0.00094\,T^2 + 0.049\,T - 0.552)$.

In addition, the extreme levels of rainfall may decrease the immature mosquitoes by flushing out larvae and breeding sites [4]. Thus, assumed that a quadratic relationship between Rainfall R and the daily survival probabilities of immature mosquitoes $p_i(R)$ is defined by [31] as $p_i(R) = \frac{4 * P_i^*}{R_L^2} R(R_L - R)$, where R_L is the rainfall limit beyond which breeding site get flushed out and no immature mosquitoes survive and P_i^* is the maximum daily survival probability of each stage i.

Adult mosquitoes seeking host for meal might die at a temperature-dependent rate μ_{VT}. Survivors seeking meal acquire malaria at a rate Λ_V which depends on the infectiousness of

the human population, since study mainly performed on human host.

$$\Lambda_V = \frac{\epsilon(\beta_{VH} I_H + R_H \xi)}{N_H}$$

where β_{VH} and ξ are probability of infection from infectious and recovery humans to susceptible mosquitoes respectively.

When the mosquito bites an infectious human, the parasite (in the form of gametocytes) enters the survivors mosquito, and subsequently process to the infectious compartment I_V through a latent period E_V. The mosquitoes become infectious at rate σ_{VT} to humans and remain infectious for life (until they die). The population dynamics and infection process of anopheles Gambiae mosquitoes are given by the following set of ordinary differential equations.

$$\begin{cases} \dfrac{dM}{dt} = \beta_{VT} \left(1 - \dfrac{M}{K}\right)(N_V) - \mu_i M - \eta(T,R)\, M, \\ \dfrac{dS_V}{dt} = \eta(T,R)\, M - \Lambda_V S_V - S_V \mu_{VT}, \\ \dfrac{dE_V}{dt} = \Lambda_V S_V - (\mu_{VT} + \sigma_{VT})\, E_V, \\ \dfrac{dI_V}{dt} = \sigma_{VT} E_V - I_V \mu_{VT}, \end{cases} \tag{3.2}$$

Table 1: Parameters for Anopheles Gambiae Model

Description	Estimate and function form	Ref
Per capita egg deposition rate, β_{VT}	$-0.153\,T^2 + 8.61\,T - 97.7$	[27]
Immature mosquito death rate, $\mu_i(T)$	$1.0257 - 0.094\,T - 0.0025\,T^2$	[26]
Adult mosquito death rate , μ_{VT}	$-\ln(0.522 - 0.000828\,T^2 + 0.0367\,T)$	[25]
Adult mosquito birth rate, $\eta(T,R)$	$\frac{\varpi(T)p_1(R)p_2(R)p_2(T)p_3(R)}{\tau_{EA}(T)}$	[25]
The lifetime number of eggs laid, $\varpi(T)$	$\beta_{VT}/\mu_{VT})$	[25]
Daily survival probabilities of eggs, $p_1(R)$	$\frac{4*.93}{R_L^2} R(R_L - R)$	[31]
Daily survival probabilities of larva, $p_2(R)$	$\frac{4*0.25}{R_L^2} R(R_L - R)$	[31]
Daily survival probabilities of pupae, $p_3(R)$	$\frac{4*0.75}{R_L^2} R(R_L - R)$	[31]
Daily survival probabilities of larva, $p_2(T)$	$e^{-(0.00554\,T - 0.06737)}$	[31]
Rainfall beyond which no immature stages survive, R_L	50	[26]
Duration of immature development, $\tau_{EA}(T)$	$1/(-0.00094\,T^2 + 0.049\,T - 0.552)$	[25]
Progression rate of mosquitoes, σ_{VT}	$e^{\breve{}1/(-4.41 + 1.31\,T - 0.03\,T^2)}$	[12]
Carrying capacity of larvae K	1000000	[26]

We note that the model describes a population and therefore it is very important to prove that all the state variables ($S_H(t); E_H(t); I_H(t); R_H(t); M(t); S_V(t); E_V(t)$ and $I_V(t)$) are non-negative at all times. For the biological benefit System (3.1) and (3.2) will be analyzed in a suitable feasible region $\Re$ defined by.

$$\Re = \left\{ (S_H; E_H; I_H; R_H) \in \mathbb{R}^4_+ | 0 \leq N_H(t) \leq \frac{\Gamma}{\mu_H}, (M; S_V; E_V; I_V) \in \mathbb{R}^4_+ | 0 \leq N_V(t) \leq \frac{\eta M}{\mu_{VT}} \right\}$$

If the system has non-negative initial data, then the solution will remain inside $\Re$ for all time $t > 0$. Thus we state the following lemma.

Lemma 3.1.
Given the model (3.1), suppose that $S_H(0) \geq 0, E_H(0) \geq 0, I_H(0) \geq 0, R_H(0) \geq 0, M(0) \geq 0, S_H \geq 0, E_H(0) \geq 0, I_H(0) \geq 0$ for all t. Then the solution $S_H(t)$; $E_H(t)$; $I_H(t)$; $R_H(t)$; $M(t)$; $S_V(t)$; $E_V(t)$; $I_V(t)$ of the model remain positive for all time $t > 0$. Moreover,

$$\lim_{t \mapsto \infty} N_H(t) \leq \frac{\Gamma}{\mu_H}$$

Furthermore, if

$$N_H(0) \leq \frac{\Gamma}{\mu_H}$$

then

$$N_H(t) \leq \frac{\Gamma}{\mu_H}$$

In particular, the region is positively invariant.
Proof. We argue by contradiction. Let us assume that the set X below is bounded.

$$X = \{T \geq 0 : S_H > 0, E_H > 0, I_H > 0, R_H > 0; M > 0; S_V > 0; E_V > 0; I_V > 0, \forall\, 0 \leq t \leq T\}.$$

Then X has a supremum T. Since $(S_H(t), E_H(t), I_H(t), R_H(t), M(t), S_V(t), E_V(t)$ and $I_V(t))$ are continuous, we have $T > 0$. From the first equation of the model (3.1) we have

$$\frac{dS_H}{dt} = \Gamma - \Lambda_H S_H + \kappa R_H - \mu_H S_H.$$

Let $B(t) = \exp\{\mu_H t + \int_0^t \Lambda_H(s) ds\}$, and note that $B(0) = 1$.
Then we have

$$\begin{aligned} \frac{d}{dt}[S_H(t).B(t)] &= \dot{S_H}(t).B(t) + S_H(t).\dot{B}(t) \\ &= \dot{S_H}(t).B(t) + S_H(t).B(t)(\mu_h + \Lambda_H(t)) \\ &= B(t)[\dot{S_H}(t) + S_H(t).(\mu_H + \Lambda_H(t))] \\ &= (\Gamma + \kappa R_H(t))B(t). \end{aligned} \tag{3.3}$$

Hence

$$S_H(T).B(T) - S_H(0).B(0) = \int_0^T (\Gamma + \kappa R_H(t))B(t) dt,$$

so that

$$S_H(T) = B(T)^{-1}\Big[S_H(0) + \int_0^T (\Gamma + \kappa R_H(t))B(t)\Big].$$

Note that $R_H(t) > 0$, $B(t) > 0$ for all t, and so $S_H(0) \geq 0$. Therefore $S_H(T) > 0$.
A similar reasoning on the remaining equations shows that E_H, I_H, R_H, M, S_V E_V, and I_V are always positive for $t > 0$. This contradicts T being the supremum of X
Further by adding the equations of the system (3.1) we obtain

$$\frac{dN_H}{dt} = \Gamma - \mu_H N_H(t).$$

Using a standard comparison

$$N_H(t) = \frac{\Gamma}{\mu_H} + \Big(N_H(0) - \frac{\Gamma}{\mu_H}\Big)e^{-\mu_H t}$$

Therefore,

$$\lim_{t\mapsto\infty} sup N_H(t) = \frac{\Gamma}{\mu_H}.$$

This establishes the invariance of X as claimed. □

3.2 Model fitting

In this subsection, we fit our model to data in a Bayesian framework using Markov Chain Monte Carlo (MCMC) methods. The Bayesian method combines the likelihood of the data as well as the prior distribution of the parameters of the model to obtain the posterior distribution of the parameters of the model, expressed by

$$p(\theta|Data) = \frac{p(Data|\theta)p(\theta)}{p(Data)},$$

where $p(\theta|Data)$ is the posterior, $p(Data|\theta)$ is the likelihood, $p(\theta)$ is the prior, $p(Data)$ is a normalisation constant. This allows one to make inference based on the posterior mean/ median of the parameters. The parameters driving the human model were jointly estimated by utilizing MCMC in fitR (version 0.1 [8]) package to clinical incidence data, weighted by a demographic change.

The process of parameter estimation will guide to more accurate and informative model predictions of malaria disease on these specific locations. A compartmental equation was added into the human model to account for malaria incidence cases during model fitting process. The model fitting was undertaken by using weekly malaria data of 2015 for each region under investigation (for CES and WBGZ shown in Figure 4 and 5 respectively) using MCMC. The model is run from the year 2000 to reach a steady state before being fitted to data from the year 2011, then validated with data from 2011 to 2015.

We assume that weekly malaria data were reported according to a Poisson process with reporting rate ζ. Since the reporting rate is unknown we assume it to be no larger than

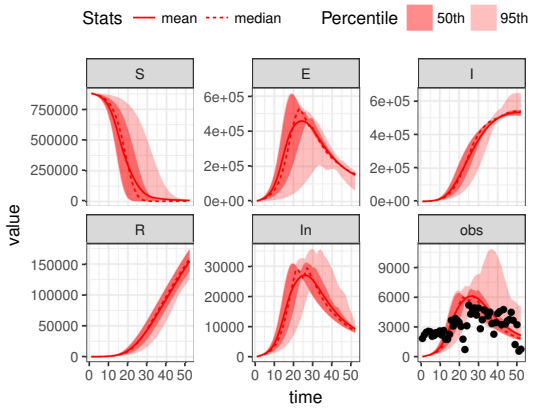

Figure 4: Illustration of the model fitting and the trajectory simulation, the model assessment (line) run against data (dots) of CES for 2015 attached with the parameters estimated during fitting process in Table 2.

85%. We assume that $x_{ij}(i = 1, \ldots, n; j = 1, \ldots, m)$ are the observed weekly malaria incidence cases for state j during week i. We used uniform distributions to model the prior belief regarding the parameters. During this fitting process the model parameters β_{HV}, ϵ_j, γ, τ, ν, and κ were estimated and presented in table 2. These parameters were assumed to be constant and were jointly estimated by utilizing fitR (version 0.1 [8]) to obtain posterior samples 10000 iterations and a burn-in of 1000 iterations used for three chains. The confidence intervals produced in Figure 4 and 5 was a 95% confidence intervals with accepting rate of 0.22 and 0.178 for CES and WBGZ respectively.

Table 2: Parameters for the human transmission model

Description	Est for CES	Est for WBZ
Human natural death rate, μ_H	0.00006166	0.00006166
Population size, N	882846	266745
Mosquito biting rate, ϵ	26.065	18.895
Probability of infection from infected mosquito , β_{HV}	0.6458	0.7458
lost of immunity, κ	1/25	1/36
Rate of progression of humans from E to I, σ_H	1/16	1/13
Proportion of infected population receving treatment π	0.84978	0.92258
All elimination half-life, ν	7	5
Treatment seeking period, τ	4	3
Natural recovery period, γ	166	152
Clinical death rate of humans due to malaria, δ	0.0027	0.0011
Probability of infection from Infected human , β_{VH}	0.48	0.48
probability of infection from recovery human, ξ	0.06	0.0028

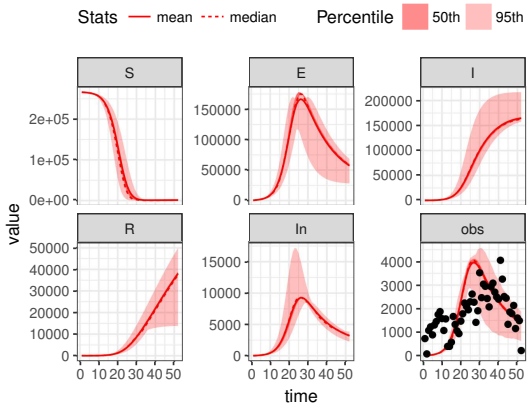

Figure 5: Illustration of the model fitting and the trajectory simulation, the model assessment (line) run against data (dots) of WBGZ for 2015 attached with the parameters estimated during fitting process in Table 2.

4 Model analysis

The existence of a trivial equilibrium of the model (3.1) and (3.2) will be explored by setting the equations equal to zero. Consider the following disease free model:

$$\begin{aligned} \frac{dS_H}{dt} &= \Gamma - \mu_H S_H \\ \frac{dM}{dt} &= \beta_{VT}\left(1-\frac{M}{K}\right)S_V - \mu_i(T)M - \eta(T,R)M \\ \frac{dS_V}{dt} &= \eta(T,R)M - \mu_{VT}S_V \end{aligned} \tag{4.4}$$

This system has two equilibrium points:

i. The vector free equilibrium point $E_{00} = \left(\frac{\Gamma}{\mu_H}, 0, 0\right)$ and

ii. The vector endemic (disease free) equilibrium point

$$E_0 = \left(\frac{\Gamma}{\mu_H}, \frac{K\mu_{VT}\left(\eta(T,R)+\mu_i(T)\right)(\Theta-1)}{\eta(T,R)\beta_{VT}}, \frac{K\mu_{VT}\left(\eta(T,R)+\mu_i(T)\right)(\Theta-1)}{\beta_{VT}\mu_{VT}}\right)$$

where $\Theta := \dfrac{\eta(T,R)\beta_{VT}}{\mu_{VT}\left(\mu_i(T)+\eta(T,R)\right)}$.

Note that the vector endemic equilibrium is positive if and only if $\Theta > 1$.

Next, we show that Θ is the basic offspring number.

Consider the submodel of (4.4) formed by the equations of the vector only, that is

$$\begin{array}{rcl} \dfrac{dM}{dt} & = & \beta_{VT}\left(1-\frac{M}{K}\right)S_V-\mu_i\left(T\right)M-\eta\left(T,R\right)M \\ \dfrac{dS_V}{dt} & = & \eta\left(T,R\right)M-\mu_{VT}S_V \end{array} \tag{4.5}$$

Let $\mathcal{G}=\begin{pmatrix}\beta_{VT}S_V\\0\end{pmatrix}$ denote the vectors of new offsprings in the disease free model (4.5) and let $\mathcal{W}=\begin{pmatrix}\beta_{VT}\frac{M}{K}S_V+\mu_i\left(T\right)M+\eta\left(T,R\right)M\\-\eta\left(T,R\right)M+\mu_{VT}S_V\end{pmatrix}$ be the vector formed by the other transfers.

The next generation matrix is given by GW^{-1} where G and W are the Jacobian matrices evaluated at $(0,0)$ of $\mathcal{G}$ and $\mathcal{W}$ respectively.

Such that :

$$GW^{-1}=\begin{bmatrix}-\dfrac{\eta\left(T,R\right)\beta_{VT}}{\left(\mu_i\left(T\right)+\eta\left(T,R\right)\right)\mu_{VT}} & \dfrac{\beta_{VT}}{\mu_{VT}}\\0&0\end{bmatrix}.$$

The basic offspring number, Θ, is given by the spectral radius of GW^{-1}.

We obtain

$$\begin{aligned}\Theta=\rho\left(GW^{-1}\right) &= \max\left(0,\left|-\frac{\eta\left(T,R\right)\beta_{VT}}{\left(\mu_i\left(T\right)+\eta\left(T,R\right)\right)\mu_{VT}}\right|\right)\\ &= \frac{\eta\left(T,R\right)\beta_{VT}}{\left(\mu_i\left(T\right)+\eta\left(T,R\right)\right)\mu_{VT}}.\end{aligned}$$

Evaluating the Jacobian matrix at the vector free equilibrium, we obtain:

$$J_0=\begin{bmatrix}-\mu_H & 0 & 0\\0 & -\mu_i\left(T\right)-\eta\left(T,R\right) & \beta_{VT}\\0 & \eta\left(T,R\right) & -\mu_{VT}\end{bmatrix}$$

The characteristic polynomial of the Jacobian matrix evaluated at E_{00}, is

$$\left(\mu_H+z\right)\left(z^2+\left(\eta\left(T,R\right)+\mu_i\left(T\right)+\mu_{TV}\right)z+\mu_{TV}\left(\eta\left(T,R\right)+\mu_i\left(T\right)\right)\left(1-\Theta\right)\right)$$

Hence, E_{00} is locally assumptotically stable if and only if $\Theta<1$.

Similarily, the Jacobian matrix at the vector endemic equilibrium

$$J_1=\begin{bmatrix}-\mu_H & 0 & 0\\0 & -\frac{\beta_{VT}S_{V0}}{K}-\mu_i\left(T\right)-\eta\left(T,R\right) & \beta_{VT}\left(1-\frac{M_0}{K}\right)\\0 & \eta\left(T,R\right) & -\mu_{VT}\end{bmatrix}$$

The characteristic polynomial of the Jacobian matrix evaluated at E_0, is

$$\left(\mu_H+z\right)\begin{bmatrix}Kz^2+\left(\eta\left(T,R\right)K+\mu_i\left(T\right)K+K\mu_{VT}+\beta_{VT}S_{V0}\right)z\\+\beta_{VT}\eta\left(T,R\right)M_0+S_{V0}\beta_{VT}\mu_{VT}+K\left(\eta\left(T,R\right)\mu_{VT}+\mu_i\left(T\right)\mu_{VT}\right)\left(1-\Theta\right)\end{bmatrix}$$

Hence, E_0 is locally assumptotically stable if $\Theta > 1$.

Next, we calculate the basic reproduction number. The basic reproduction number, denoted by $\mathcal{R}_0$, plays a vital role in the propagation of the relevant epidemic. It gives condtions on when a disease free equilibrium exists or is unstable. The threshold quantity, $\mathcal{R}_0$, is defined (see [37] for instance) as the average number of new infections that occur when one infective individual is introduced into a completely susceptible human population. Here, the $\mathcal{R}_0$ of the model (3.1) and (3.2) is establish in Lemma 3.2 using the next generation matrix concomitant with disease free equilibrium.

Lemma 3.2. *The basic reproduction number of the system* (3.1) *and* (3.2) *is*

$$\mathcal{R}_0 = \sqrt{\frac{\epsilon^2 \sigma_{VT} \sigma_H \mu_H \beta_{VH} \beta_{HV} K \left(\xi\,\rho + \kappa + \mu_H\right) \left(\mu_i\left(T\right) + \eta\left(T,R\right)\right) \left(\Theta - 1\right)}{\Gamma \beta_{VT} \left(\rho + \delta + \mu_H\right) \left(\sigma_H + \mu_H\right) \left(\kappa + \mu_H\right) \left(\sigma_{VT} + \mu_{VT}\right) \mu_{VT}}}.$$

Proof.

Let $\mathcal{F}$ denote the vectors of new infection in the full model and let $\mathcal{F}$ and $\mathcal{V}$ be the vector formed by the other transfers. We have

$$\mathcal{F} = \begin{bmatrix} \frac{\epsilon\,\beta_{HV} I_V S_H}{S_H + E_H + I_H + R_H} \\ 0 \\ 0 \\ \frac{\epsilon(\xi\,R_H + \beta_{VH}\,I_H) S_V}{S_H + E_H + I_H + R_H} \\ 0 \end{bmatrix}, \mathcal{V} = \begin{bmatrix} \left(\sigma_H + \mu_H\right) E_H \\ -\sigma_H E_H + \left(\rho + \delta + \mu_H\right) I_H \\ -\rho\, I_H + \left(\kappa + \mu_H\right) R_H \\ \left(\sigma_{VT} + \mu_{VT}\right) E_V \\ \mu_{VT}\, I_V - E_V \sigma_{VT} \end{bmatrix}$$

The next generation matrix is given by FV^{-1} where $F = \partial \mathcal{F}_{E_0}$ and $V = \partial \mathcal{V}_{E_0}$ denote the jacobian matrices of $\mathcal{F}$ and $\mathcal{V}$ evaluated at E_0. We obtain:

$$FV^{-1} = \begin{bmatrix} 0 & 0 & 0 & \frac{\epsilon\,\beta_{HV}\sigma_{VT}}{(\sigma_{VT}+\mu_{VT})\mu_{VT}} & \frac{\epsilon\,\beta_{HV}}{\mu_{VT}} \\ 0 & 0 & 0 & 0 & 0 \\ 0 & 0 & 0 & 0 & 0 \\ A & B & C & 0 & 0 \\ 0 & 0 & 0 & 0 & 0 \end{bmatrix}$$

where

$$\begin{aligned} A &= \frac{\beta_{HV} K \epsilon \sigma_H \mu_H \left(\eta\left(T,R\right) + \mu_i\left(T\right)\right) \left(\kappa + \mu_H + \xi\rho\right) \left(\Theta - 1\right)}{\Gamma \beta_{TV} \left(\sigma_H + \mu_H\right) \left(\delta + \rho + \mu_H\right) \left(\kappa + \mu_H\right)} \\ B &= \frac{\beta_{HV} K \epsilon \mu_H \left(\eta\left(T,R\right) + \mu_i\left(T\right)\right) \left(\kappa + \mu_H + \xi\rho\right) \left(\Theta - 1\right)}{\Gamma \beta_{TV} \left(\delta + \rho + \mu_H\right) \left(\kappa + \mu_H\right)} \\ C &= \frac{\epsilon\,\beta_{VH} \xi\,\mu_H K \left(\mu_i\left(T\right) + \eta\left(T,R\right)\right) \left(\Theta - 1\right)}{\Gamma\,\beta_{VT} \left(\kappa + \mu_H\right)} \end{aligned}$$

The eigenvalues of FV^{-1} are $0, -\sqrt{\frac{\epsilon \beta_{HV} \sigma_{TV} A}{\mu_{TV}\left(\sigma_{TV} + \mu_{TV}\right)}}$ and $\sqrt{\frac{\epsilon \beta_{HV} \sigma_{TV} A}{\mu_{TV}\left(\sigma_{TV} + \mu_{TV}\right)}}$.
Therefore the basic reproduction number for the system is as claimed. □

According to a general result established in [37], we conclule that the disease-free equilibrium E_0 of the model (3.1) and (3.2) is locally asymptotically stable if $\mathcal{R}_0 < 1$, and unstable if $\mathcal{R}_0 > 1$.

We will now analyse the sensitivity index of $\mathcal{R}_0$ with respect to the parameters V, χ, T and R according to the definition below.

Definition 1. *The sensitivity index of $\mathcal{R}_0$ with respect to a parameter p is given by*

$$\Gamma^p_{\mathcal{R}_0} = \frac{\partial \mathcal{R}_0}{\partial p}\frac{p}{\mathcal{R}_0}.$$

The sensitivity index of $\mathcal{R}_0$ with respect to χ and V are illusrated in Figure 6 and given by

$$\mathcal{S}_V := \frac{\partial R_0}{\partial V}\frac{V}{R_0} = \frac{\chi V}{\chi V - 1} = \frac{\partial R_0}{\partial \chi}\frac{\chi}{R_0}$$

With regard to the sensitivity index of $\mathcal{R}_0$ to T and R, we observe from Figure 7 that when the rainfall is averaging 50 mm, temperatures below 33.7°C have a negative impact on $\mathcal{R}_0$ with the proportional decrease in $\mathcal{R}_0$ declining with increasing temperatures to reach zero when the temperature reaches 33.7°C. Beyond this value, the temperature starts having a positive impact on $\mathcal{R}_0$. We also observe that when the rainfall is equal to 70 or 80 mm, temperatures below 28.8 °C have a positive impact on $\mathcal{R}_0$. Moreover, as temperature increases, the proportional increase in $\mathcal{R}_0$ declines to become equal to zero when the temperature reaches 28.80C. Above 28.8°C, any increase in temperature leads to a decline in $\mathcal{R}_0$ with the proportional decline in $\mathcal{R}_0$ increasing as temperature increases.

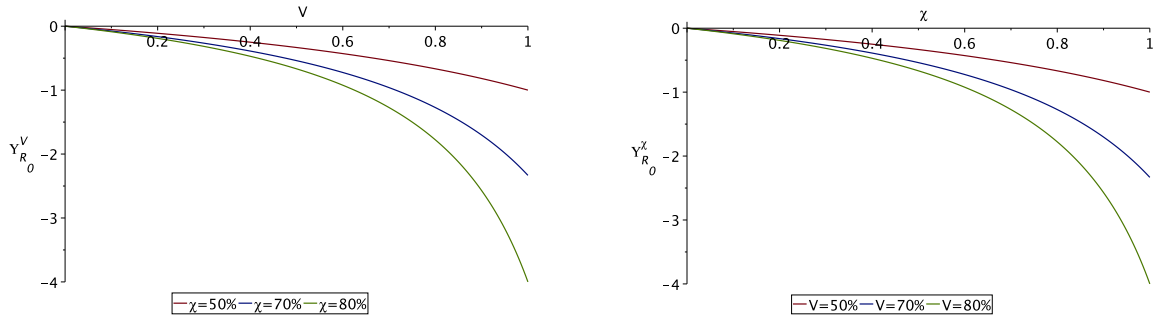

Figure 6: Sensitivity index of $\mathcal{R}_0$ with respect to χ and V.

5 Result and Discussion

In this paper, we presented and analyzed a mathematical model in order to explore the impact of climatic conditions on malaria infections in two distinct regions of South Sudan. Model fitting via MCMC and the trajectory simulation of human dynamics were carried out. We derived the basic reproduction number $\mathcal{R}_0$ and examined the model for the existence

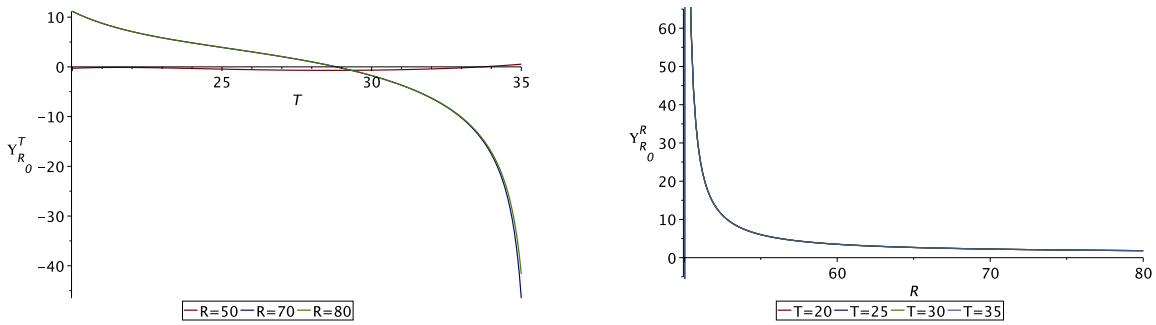

Figure 7: Sensitivity index of $\mathcal{R}_0$ with respect to R and T.

of vector free and disease-free equilibrium points. We have discussed the stability of the diseases–free equilibrium of the model. We then performed a sensitivity analysis of $\mathcal{R}_0$ with respect to temperature and precipitation was performed. Temperature and rainfall define the mosquito life cycle and control mosquito activity, including egg diapause. Mosquitoes have been described as cold-blooded insects which are unable to regulate temperature on their own [10, 27]. This means that their body temperature is dependent on the atmosphere in which they live.

Yet, temperature's role in exacerbating malaria and the impact of weather and rainfall has been a controversial topic in recent years. Here Figure 9 (D) illustrates, the occurrence of Mosquito abundance when the mean monthly temperature and rainfall values lie in the ranges of 25 -30°C and 20 -30 mm respectively. The results demonstrate that mosquitoes are active once temperatures are consistently above 10°C, and are sedentary when temperatures reach 35°C. The results also indicate that the survivor probability of immature mosquitoes (eggs, larvae, pupae) could be reduced by low or excessive levels of rainfall (see Figure 9 (C)). Furthermore, the results suggest that daily rainfall in the range of 17–20 mm and temperatures in the range of 20°C to 35°C are ideal for progression of mosquitoes, and hence, for the spread of malaria. Our results also highlight the significant role of warmer temperatures in the aggravation of the disease, acting in the same direction of [2].

It can also be observed that the immature mosquitoes are more sensitive to temperatures at 25°C than the mature mosquitoes. These patterns were incorporated into a deterministic model of Anopheles gambiae population dynamics, in order to gain insight into the abundance of mosquitoes, thus providing an effective tool for control strategies in combating the spread of malaria. Temperatures in the range of 25°C to 30°C are more suitable for the progression of mosquitoes at all stages in their life-cycle (shown in Figure 8). This indicate that, mosquito dynamics are strongly shaped by warm weather ecology which appears to be consistent with other studies [5, 28, 31, 26, 33]. Accordingly, understanding the effect of climate change on malaria transmission dynamics is crucial in designing effective anti-malaria measures.

A model with a seasonal averaged climate in two study region is analyzed regarding malaria transmission. For example, nvestigated the sensitivity of $\mathcal{R}_0$ to average monthly

Table 3: Estimate of basic reproduction number $\mathcal{R}_0$ against Mean Rainfall (MR) and Average Temerature (AT) using parameter values from Table 2

	CES			WBGZ		
Month	AT(C)	MR(mm)	$\mathcal{R}_0$	AT(C)	MR(mm)	$\mathcal{R}_0$
Jan	38	6.1	1.11414	26.8	0	0.971627
Feb	38	27.9	3.89315	28.5	0	0.747225
Mar	38	31.4	3.58896	30.7	6	6.315132
Apr	37	72.2	4.62567	31.1	21	20.506707
May	34	132	8.62933	29.5	87	19.370367
Jun	32	146	14.27812	27.4	107	20.816907
Jul	30	304.5	20.89713	26.1	152	13.340053
Aug	31	91	17.32905	26.2	169	10.366855
Sep	32	93.1	14.27812	26.6	131	12.509831
Oct	33	111	11.70291	27.5	78	30.831914
Nov	35	28.3	7.73881	27.3	6	11.329622
Dec	36	15	5.09080	26.5	0	1.011970

temperature and rainfall data that are presented in Table 3. In numerical calculation of $\mathcal{R}_0$, we assume 50 mm of rain will flushed out mosquitoes from their breeding site, therefore the precipitation is considered during the peak period to be less than 50 mm in $\mathcal{R}_0$ approximation. From April $\mathcal{R}_0$ is overestimated due to rainfall that increase above the average of 50 mm, we instead used a fix value of 40 mm. Our results indicate that $\mathcal{R}_0$ varies monotonically with the influence of rainfall and temperature. We note in the results that the reproduction number value increases during the peak period of the rainy season starting from March to October in CES. The onset of increased transmission intensity between July and September can be explained by the seasonal increase in A. Gambiaes and a weakening of the clinical immunity of individuals. A similar pattern in transmission applied to WBGZ but with low disease intensity compared to CES which is most likely owing to the climate differences. Findings of this study are in agreement with other studies [2, 29] that demonstrate disease behavior changes with changes of local climate. These findings also suggest that the factor of climate can be a decisive determinant of malaria spatial distribution throughout the country.

Furthermore, in the case of WBGZ, the mosquito birth rate tends towards zero when the rainfall is minimal from November to February, hence, the reproduction number tends to zero. After February it begins to increase, reaching a peak in the months from June to October. This pattern, along with mean local rainfall and temperature shown in Figure 7, confirms our hypothesis that malaria transmission is influenced by weather and rainfall, since the disease is more prevalent in the favourable climate of CES than it is in WBGZ. This study, therefore, highlights the difference between the high transmission rate in tropical climates (CES) and the low transmission in hot semi-arid climates (WBGZ), a difference which further coincides with the two distinct but adjacent cohorts of mesoendemic seasonal

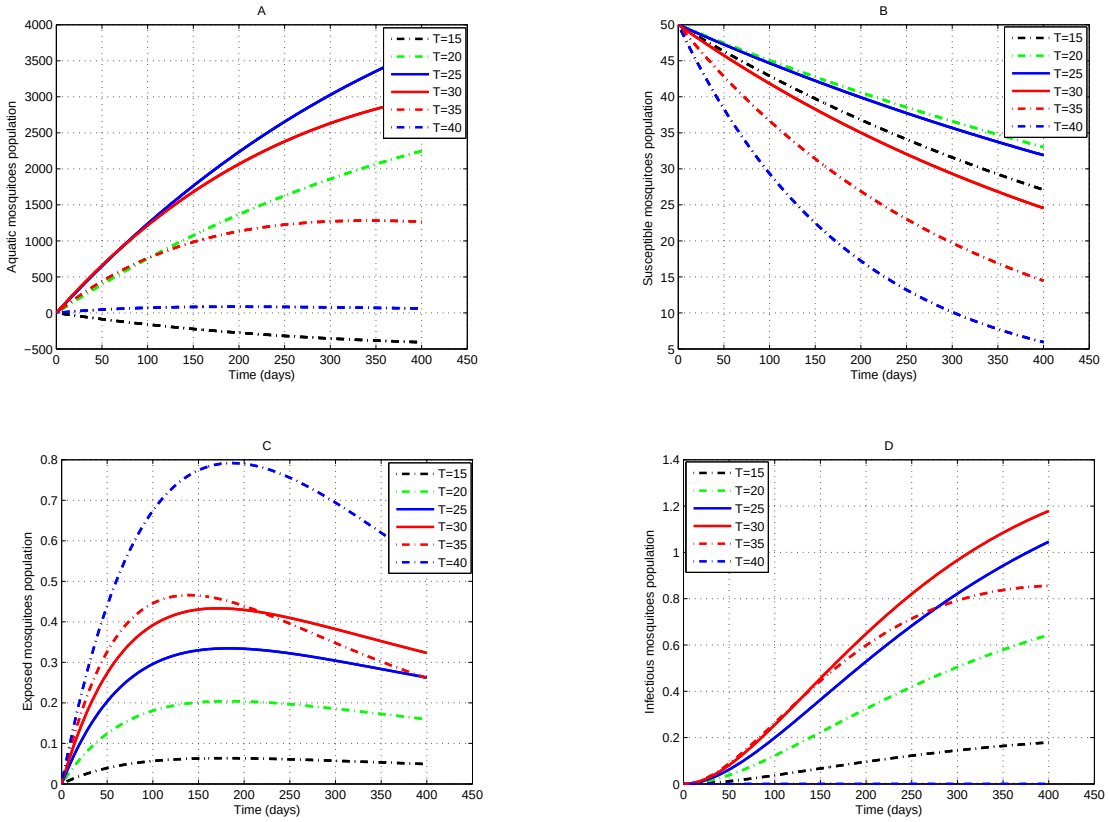

Figure 8: Simulation of the model, using parameter values in Table 1, assess the impact of various temperature values on the population dynamics of the mosquito

and holoendemic perennial malaria transmission [29].

These results point to the importance of incorporating detailed mosquito bionomics with climate-dependence into models for predicting the risk for malaria. These models can also be used to understand the possible changes in malaria prevalence in regions experiencing climate change: in the case of South Sudan, changes to regional climates, including changes in rainfall and temperature patterns, will alter the variability of malaria cases.

Using a realistic representation of the coupled mosquito–human model will aid to understand the dynamics of malaria over the study region. Noting that parameters such as mosquito size and mosquito bite assumption rate can influence the realization of disease behavior [21]. Hence, it was stimulating to validate our model with field data and implement parameter estimation to increase realism. Therefore, the mosquito model that provides a detailed mosquito bionomics with climate-dependence in line with several studies [5, 12, 11, 39] for predicting the risk for malaria is carried out. Moreover, our research sought to filter out the climatic factors affecting the force of infection which consist of infectious bites, and hence altered it with the effect of intervention coverage, unlike the studies [4, 18, 26, 38]. As the measurement of entomological inoculation rate (EIRs, measuring the number of infectious

bites per person per year) is related to the measure of infection intensity, therefore it should be estimated during the model fitting process with the effect of intervention coverage given the disease incidence cases.

The availability of mosquito climate-based models and realistic parameter values determined through data fitting process allows researchers to predict more reliably disease transmission dynamics. We hope that this study improves understanding of the climate role as the first step in providing information that may lead to significant changes in the way that the disease is transmitted in these regions to incorporate the effective interventions.

6 Conclusion

We propose a host-mosquito model for malaria transmission in two climatic regions in South Sudan. We used MCMC to fit the model to malaria data from these two regions. The validated model is further used to calculate the basic reproductive number and assess its sensitivity to climate factors. The basic reproductive number is used to provide a numerical basis $\mathcal{R}_0$ is used to provide a numerical basis for further refinement and prediction of the impact of climate variability on malaria transmission intensity in two regions (i.e. CES and WBGZ).

The results in these both regions indicate that malaria trend follows the climate pattern with its epidemiological peak between February-December and between March-November when temperature and rainfall progressively increase in the CES and WBGZ respectively. The findings also demonstrated that disease is more effective and severe in tropical (CES) region than in a hot semi-arid (WBZ) region due to climate conditions. Hence, we concluded that this study which analyses observed phenomena also seeks ways of informing decision making together with ideas for the continuation of malaria control in South Sudan. A model calibration was one of the main contributions that this study has achieved, complemented with the realistic representation of Anopheles Gambiae population dynamics to gain insight into the abundance of mosquitoes and hence the course of the epidemic.

However, malaria is a complex disease that can reemerge from other factors such as socioeconomic situation and population movement which need to be incorporated in studying malaria transmission. These aspects are worthy of attention in future studies.

Acknowledgments: The authors wish to thank Robert Snow for the valuable advice provided at the early stages of this work. They are also grateful to Thomas Ujjiga for availing the data used in this research. Abdulaziz Mukhtar wishes to acknowledge the support of the DST-NRF Centre of Excellence of Mathematical and Statistical Sciences (CoE-MaSS) towards this research. Rachid Ouifki would like to thank the DST/NRF SARChI Chair in Mathematical Models and Methods in Bioengineering and Biosciences for its financial support. Opinions expressed and conclusions arrived at, are those of the authors and are not necessary to be attributed to the CoE.

7 Supporting information

Mosquitoes cycle development against climate factor

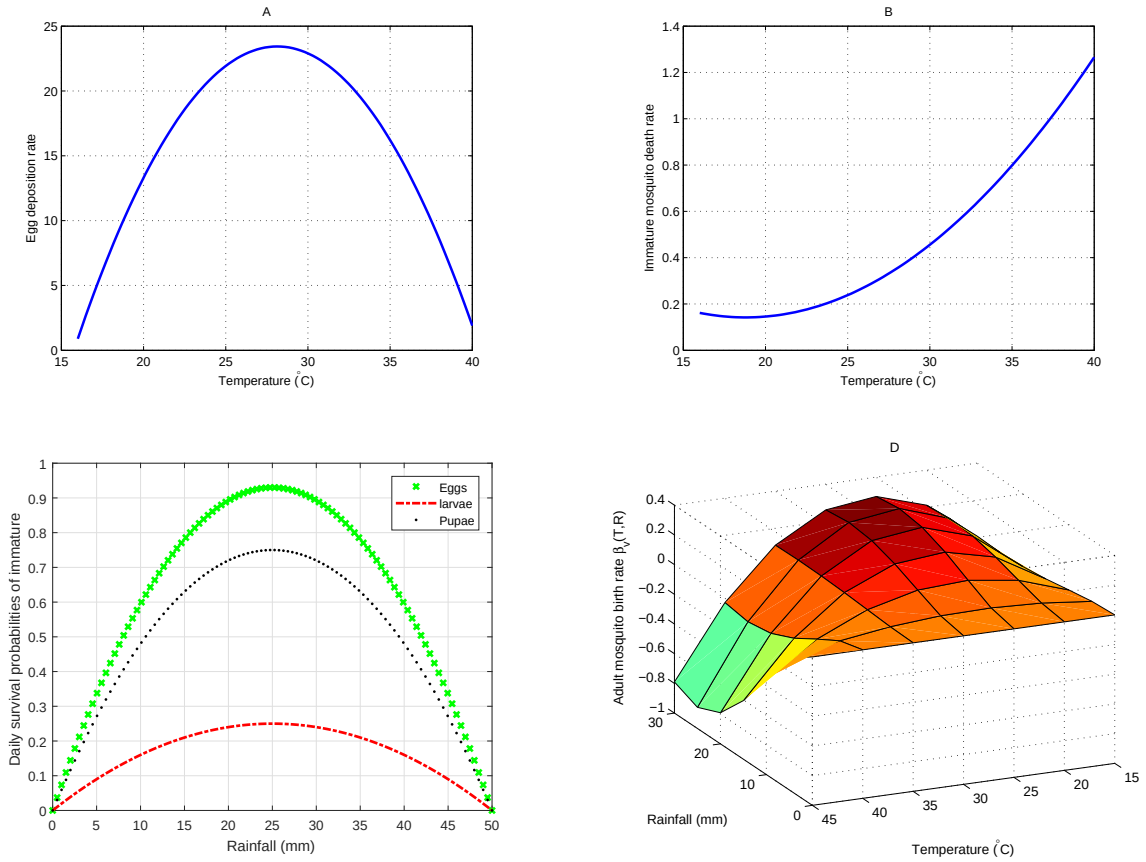

Figure 9: Simulation of model parameter function, showing mosquitoes cycle development against various values of mean monthly temperature in the range of 15- 40°C and rainfall in the range of 0-50 mm, using parameter fuctions in Table 1, (A) dependence of eggs deposition rate process on temperature (B) dependence of the daily survival probability of mosquito during aquatic stages on temperature (C) the per-capita death rate of mosquito during aquatic stages depend on temperature (D) the per-capita maturation rate of pupae (into adult mosquitoes) as a function of rainfall and temperature.

References

[1] A. Abdelrazecy and A. B. Gumely. Mathematical analysis of a weather-driven model for the population ecology mosquitoes. *Mathematical Bioscience and Engineering*, **15** (2018) 57-93.

[2] G. J. Abiodun, R. Maharaj, P. Witbooi and K. O. Okosun. Modelling the influence of temperature and rainfall on the population dynamics of Anopheles arabiensis. *Malaria Journal*, **15** (2016); DOI 10.1186/s12936-016-1411-6

[3] D. Alonso, M. J. Bouma and M. Pascual. Epidemic malaria and warmer temperatures in recent decades in an East African highland. *Proceedings of the Royal Society of London B: Biological Sciences*, **278** (2011): 1661-1669.

[4] L. M. Beck-Johnson, W. A. Nelson, K. P. Paaijmans, A. F. Read, M.B. Thomas, O. N. Björnstad. The Effect of Temperature on Anopheles Mosquito Population Dynamics and the Potential for Malaria Transmission. *PLoS ONE*; **8**; (2013) doi:10.1371/journal.pone.0079276.

[5] L. M. Beck-Johnson, W. A. Nelson, K. P. Paaijmans, A. F. Read, M.B. Thomas, O. N. Björnstad. The importance of temperature fluctuations in understanding mosquito population dynamics and malaria risk. *Royal Society Open Science*, **4** (2017) DOI:10.1098/rsos.160969.

[6] J. I. Blanford, S. Blanford, R. G. Crane, M. E. Mann, K. P. Paaijmans, K. V. Schreiber, and M. B. Thomas. Implications of temperature variation for malaria parasite development across Africa. *Scientific Reports* **3**; (2013) doi:10.1038/srep01300.

[7] at https://en.climate-data.org/.

[8] Camacho A, Funk S. FitR: Tool box for fitting dynamic infectious disease models to time series. (2017) Version 0.1 Available from: https://github.com/sbfnk/fitR.

[9] E. Chanda, C.D Remijo, H. Pasquale, S.P. Babab and R.L. Lako. Scale-up of a programme for malaria vector control using long-lasting insecticide-treated nets: lessons from South Sudan. *Bulletin World Health Organization*, **92** (2014); 290-296.

[10] C. Christiansen-Jucht, K. Erguler, C. Y. Shek , M. G. Basáñez and P. E. Parham. Modelling Anopheles gambiae s.s. Population Dynamics with Temperature- and Age-Dependent Survival. *International Journal of Environmental Research and Public Health*. **12**, (2015) 5975-6005.

[11] D. A. Ewing, C. A. Cobbold, B. V. Purse, M. A. Nunn and S. M. White. Modelling the effect of temperature on the seasonal population dynamics of temperate mosquitoes. *Journal of Theoretical Biology*, **400**; (2016) 65–79.

[12] M. Craig, D. Le Sueur, and B. Snow. A climate-based distribution model of malaria transmission in sub-Saharan Africa. *Parasitology Today*, **15** (1999); 105–111.

[13] N. Chitnis, T. Smith, R. Steketee. A mathematical model for the dynamics of malaria in mosquitoes feeding on a heterogeneous host population. *J Biol Dyn*,**2** (2008); 259–85.

[14] M.B. Eyobo, A.C. Awur, G. Wani, A. Julla, C.D. Remijo, B. Sebit, R. Azairwe, O. Thabo, E. Bepo, R.L. Lako, L. Riek and E. Chanda. Malaria indicator survey 2009, South Sudan: baseline results at household level. *Malaria Journal*, **13** (2014); 13-45.

[15] O. Ghasemi, M. L. Lindsey, T. Yang, N. Nguyen, Y. Huang and Y. Jin. Bayesian parameter estimation for nonlinear modelling of biological pathways. *BMC Systems Biology* **5**, (2011), DOI: 10.1186/175205095S3S9.

[16] M. B. Hoshen, A.P. Morse. A weather-driven model of malaria transmission. *Malaria Journal*, (2004); DOI:10.1186/1475-2875-3-32.

[17] S. S. Imbahale, K. P. Paaijmans, W. R. Mukabana, R. van Lammeren, A. K. Githeko and W. Takken. A longitudinal study on Anopheles mosquito larval abundance in distinct geographical and environmental settings in western Kenya.*Malaria Journal*, **10** (2011), DOI.10.1186/1475-2875-10-81.

[18] F. M. M. Kakmeni, R. Y. Guimapi, F. T. Ndjomatchoua, S. A. Pedro, J. Mutunga and H. E. Tonnang. Spatial panorama of malaria prevalence in Africa under climate change and interventions scenarios. *International journal of health geographics* **17** (2018) 2.

[19] A. Le Menach, S. Takala, F. E. McKenzie, A. Perisse, A. Harris, A. Flahault and D. L Smith. An elaborated feeding cycle model for reductions in vectorial capacity of night-biting mosquitoes by insecticide-treated nets. *Malaria Journal* **10** (2007), 6:10 doi:10.1186/1475-2875-6-10

[20] S.W. Lindsay, M.H. Birley. Climate change and malaria transmission. *Annals of Tropical Medicine and Parasitology*, **90** (1996);573-588.

[21] T. M. Lunde, D. Korecha, E. Loha, A. Sorteberg and B. Lindtjørn. A dynamic model of some malaria-transmitting anopheline mosquitoes of the Afrotropical region. I. Model description and sensitivity analysis. *Malaria Journal* **12** (2013) 28.

[22] W. J. M. Martens, L.W. Niessen, J. Rotmans, A.J. Mcmichael. Potential impacts of global climate change on malaria risk. *Environmental Health Perspectives*, **103** (1995); 458-464.

[23] E. M. Malik and O. Khalafalla. Malaria in Sudan: past, present and the future. *Gezira Journal of Health Sciences*, *1* (2004) 47.

[24] B. Moonen,J. M. Cohen, R.W. Snow, L. Slutske, C. Drakeley, D. L. Smith, R. R. Abeyasinghe, M. H. Rodriguez, R. Maharaj, M. Tanner and G. Targett. 'Operational strategies to achieve and maintain malaria elimination. *The Lancet*, **376** (2010), 1592-1603.

[25] E. A. Mordecai. Optimal temperature for malaria transmission is dramatically lower than previously predicted. *Ecology Letters*, **16** (2013) 22–30 .

[26] E. T. Ngarakana-Gwasira, C. P. Bhunu, M. Masocha, and E. Mashonjowa. Assessing the role of climate change in malaria transmission in Africa. *Malaria Research and Treatment* (2016) DOI:10.1155/2016/7104291.

[27] K. Okuneye , A. B. Gumel. Analysis of a temperature- and rainfall-dependent model for malaria transmission dynamics. *Mathematical Biosciences*, **287** (2017) 72-92.

[28] K. O. Okuneye, A. Abdelrazecy and A. B. Gumel. Mathematical analysis of a weather driven model for the population ecology of mosquitoes. *Mathematical Biosciences and Engineering* **15** (2017) 57-93. .

[29] K.P. Paaijmans, S. Blanford, A.S. Bell, J.I. Blanford, A. F. Read, and M.B. Thomas. Influence of climate on malaria transmission depends on daily temperature variation. *Proceedings of the National Academy of Sciences*, **107** (2010), 15135-15139.

[30] P.E Parham and E. Michael. Modeling the effects of weather and climate change on malaria transmission. *Environmental health perspectives*, **118** (2010); 620-626.

[31] P.E Parham and E. Michael. Modeling climate change and malaria transmission. *Advance in Expermintal Medicine and Biology*, **673** (2010); 184-199.

[32] H. Pasquale, M. Jarvese, A. Julla, C. Doggale, B. Sebit, M.Y. Lual, S.B. Baba and E. Chanda. Malaria control in South Sudan, 2006-2013: Strategies progress and challenges. *Malaria Journal*, **12** (2013) DOI: 10.1186/1475-2875-12-374.

[33] L. L. M. Shapiro, S. A. Whitehead, and M. B. Thomas. Quantifying the effects of temperature on mosquito and parasite traits that determine the transmission potential of human malaria. *PLoS Biology*, **15** (2017) DOI:10.1371/journal.pbio.2003489.

[34] http://www.aljazeera.com/indepth/features/2015/12/malaria-outbreak-south-sudan-151229092502839. 4 January 2016.

[35] South Sudan Statistical Yearbook (2011), National Bureau of Statistics (NBS)

[36] A. Tran, G. L'Ambert, G. Lacour, R. Benoît, M. Demarchi, M. Cros, P. Cailly, M. Aubry-Kientz, T. Balenghien and P. Ezanno. A rainfall-and temperature-driven abundance model for Aedes albopictus populations. *International Journal of Environmental Research and Public Health*, **10** (2013), 1698-1719.

[37] P. Van den Driessche, J. Watmough, Reproduction numbers and sub threshold endemic equilibria for compartmental models of disease transmission. *Mathematical Biosciences*, **180** (2002) 29-48.

[38] T. K. Yamana and E. A. B. Eltahir. Projected impacts of climate change on environmental suitability for malaria transmission in West Africa. *Environ. Health Perspect* **121**; (2013) 1179-1186.

[39] T. K. Yamana, A. Bomblies and E. A. Eltahir. Climate change unlikely to increase malaria burden in West Africa. *Nature Climate Change*, **6**, (2016) 1009.

[40] H. M Yang. Malaria transmission model for different levels of acquired immunity and temperature dependent parameters vector. *Journal of Public Health*, **34** (2000); 223-31.

[41] F. Yang, Y. H. Liu, X. P Yang ,J. Xu, A. Kapke and OA. Carretero. Myocardial infarction and cardiac remodelling in mice. *Experimental Physiology*, bf 87 (2002); 547-555.